International Journal of Advanced Robotic Systems

OPEN ACCESS
ARTICLE

Adaptive Hands-On Control for Reaching and Targeting Tasks in Surgery

Regular Paper

Elisa Beretta[1*], Elena De Momi[1], Ferdinando Rodriguez y Baena[2] and Giancarlo Ferrigno[1]

1 Electronics, Information and Bioengineering Department, Politecnico di Milano, Milano, Italy
2 Mechanical Engineering Department, Imperial College, London, UK
* Corresponding author(s) E-mail: elisa.beretta@polimi.it

Received 20 November 2014; Accepted 26 January 2015

DOI: 10.5772/60130

Abstract

Cooperatively controlled robotic assistants can be used in surgery for the repetitive execution of targeting/reaching tasks, which require smooth motions and accurate placement of a tool inside a working area. A variable damping controller, based on a priori knowledge of the location of the surgical site, is proposed to enhance the physical human-robot interaction experience. The performance of this and of typical constant damping controllers is comparatively assessed using a redundant light-weight robot. Results show that it combines the positive features of both null (acceleration capabilities > 0.8m/s^2) and optimal (mean pointing error < 1.5mm) constant damping controllers, coupled with smooth and intuitive convergence to the target (direction changes reduced by 30%), which ensures that assisted tool trajectories feel natural to the user. An application scenario is proposed for brain cortex stimulation procedures, where the surgeon's intentions of motion are explicitly defined intra-operatively through an image-guided navigational system.

Keywords variable impedance controllers, surgical robotics, cooperative controller, hands-on controller, targeting task

1. Introduction

Robotic technology can be used to supplement, augment and improve human performance during the execution of tasks [1-4]. In particular, a robotic device can cooperate with humans [5] during the repetitive execution of targeting and/or reaching tasks, which require one to smoothly move a tool inside a working area and to keep it in an arbitrary, stable position with high accuracy. Transparency, which quantifies the ability of a robot to follow human movements without any human-perceptible resistive forces, is one of the major issues in the field of human robot interaction for assistance in manipulation tasks [6]. Contrarily, the ability of approaching the target with high accuracy and then keeping the tool in a stable position depends on the robot's ability to apply resistance against environmental disturbances. Nowadays, cooperatively controlled (hands-on) robotic systems are used in robotic surgery, e.g., the RIO system (Mako Surgical, now owned by Stryker Corp.) [7] and ROBODOC® (Curexo Technology)[8] for orthopaedic surgery, the ROSA™ system (MedTech, Montpellier, France) for neurosurgery [9,10] and needle insertion devices [11]. In this context, commonly performed human gestures can be described as targeting or reaching tasks.

The aim of this work is to present a variable impedance controller for enhancing human-robot interaction during cooperative surgical targeting tasks, which needs to provide intuitive guidance and varying levels of positional accuracy in the operating field, such as during brain cortex stimulation in open-skull neurosurgery. Currently performed free-hand in different phases of surgical intervention, this procedure encompasses simple gesture execution, i.e., target reaching, which must be repetitively performed throughout the procedure. An example of a simplified workflow for a standard open-skull tumour resection procedure is reported in Figure 1. Direct electrical stimulation is performed on the cortex surface following the craniotomy to determine the best access pathway and then on subcortical areas during the tissue's resection to identify the margins of the lesion to be removed. According to the practical guide for intraoperative electrical stimulation [12], the stimulation should be performed every $5mm^2$ over the entire exposed cortical area (at least three times not successively for each site). It is hypothesized that surgeon fatigue can be reduced by the introduction of a robotic assistant, which will allow, among others, the recording of the target position in order to stimulate the same point repeatedly and with high accuracy. In order to respect these clinical accuracy requirements, while increasing the transparency of the system, the surgical robotic assistant should be able to automatically adapt its dynamics in order to enhance the physical human-robot interaction during the assisted cooperative guidance task.

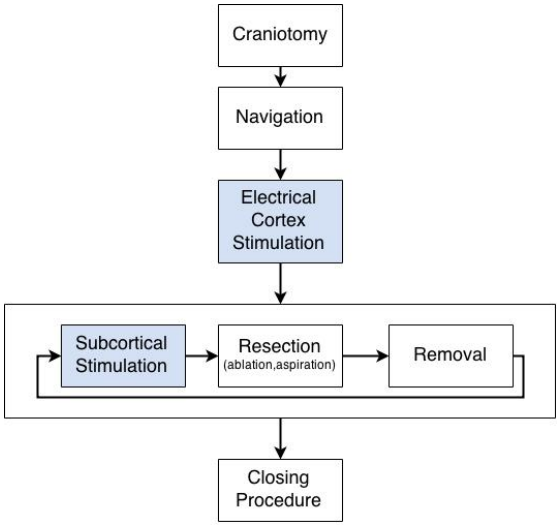

Figure 1. Block diagram of a simplified workflow for a standard open-skull neurosurgical procedure for tumour removal. The stimulation procedures (grey blocks), currently performed free-hand, are in this instance proposed to be performed with the assistance of a cooperative robotic device.

This paper is organized as follows: related work is summarized in Section 2. A variable damping controller, which aims to achieve this type of adaptable guidance control, is described in Section 3, together with details of experimental tests aimed at measuring its effectiveness. Results are presented in Section 4 and discussed in Section 5.

2. Related work

Selective and adaptive impedance control is a skilful and energy-efficient strategy humans use when learning how to interact with unstable physical environments [13]. During the past few years, adaptation criteria that mimic the human arm's behaviour have been implemented into impedance control strategies for autonomous or teleoperated robotic systems. Human-like learning controllers, derived from the minimization of instability, motion error and effort, have been developed for tasks involving interactions with unknown environments [14-17]. The question of how to adjust the compliance of the manipulator during a cooperative task has been addressed in the field of robot-learning via demonstration [18], where the human operator teaches compliance variation by physically interacting with the robot during the execution of a specific task.

Different variable impedance controllers for human-robot cooperation have been presented for surgical [8], industrial [19-21] and assistive robotics [22-26] applications. The damping factor of the impedance controller was changed with respect to a threshold, based on the speed of manipulation by direct switching [19], by time dependent functions [20] or by linear variation [21]. Conversely, robot impedance has been changed in response to the force applied by the user at the guidance contact point [8,22,23]. More intuitive and stable human-robot cooperation was accomplished when the impedance of the manipulator was modulated with respect to an estimate of the unknown human arm stiffness in [24] and/or of the human intention of motion [25]. Finally, in [26], the impedance of a meal-assistance robot was changed with respect to the end-effector position, considering a pre-defined potential field of the obstacles in the workspace around which the velocity of the robot must be restricted.

It was also shown that the reactive model of a manipulator can be approximated to a second order dynamic system, where the effect of the stiffness parameter is negligible [27], thus allowing a robotic arm to be controlled as a (simpler) damping system. A low damping coefficient allows for fast system reactions to any applied forces, while a high damping parameter is useful for preventing overshoot, reducing the virtual inertia of the system in situations where the human intention is aimed at decelerating and stopping at a particular point in the robot workspace [24].

In the current study, an autonomous adaptation control criterion is presented for enhancing the performance of a surgical hands-on robotic assistant in terms of ease of use and intuitive guidance during targeting tasks. The variable impedance approach, based on the end-effector position, is appropriate for the aforementioned surgical scenario, due to the varying accuracy and safety requirements in the operating theatre, which depend on the position of the patient and therefore also the surgical area of interest. Additionally, the impedance would not

depend on the characteristics and weight of the surgical tool, as would be the case in [22-25]. Differently from [26], where a computational demanding potential field is computed to describe an environment assumed to be static, in this work, a space variable (SV) damping criterion is presented in order to build an intra-operative "accuracy map", based on the knowledge of the surgeon's intention of motion (i.e., the position of the surgical target at the end of the reaching gesture). The performance of the SV controller is comparatively assessed with respect to two well-known impedance controllers with fixed dynamic parameters, identified as the most transparent and the optimal constant damping controllers. The experimental evaluation was carried out with a flexible joint redundant robot during predefined reaching tasks towards registered targets on a calibration board. Moreover, the applicability of the SV approach in a surgical scenario for brain cortex stimulation procedures, in which the surgical targets are not known a priori, is extensively discussed in Section 5.

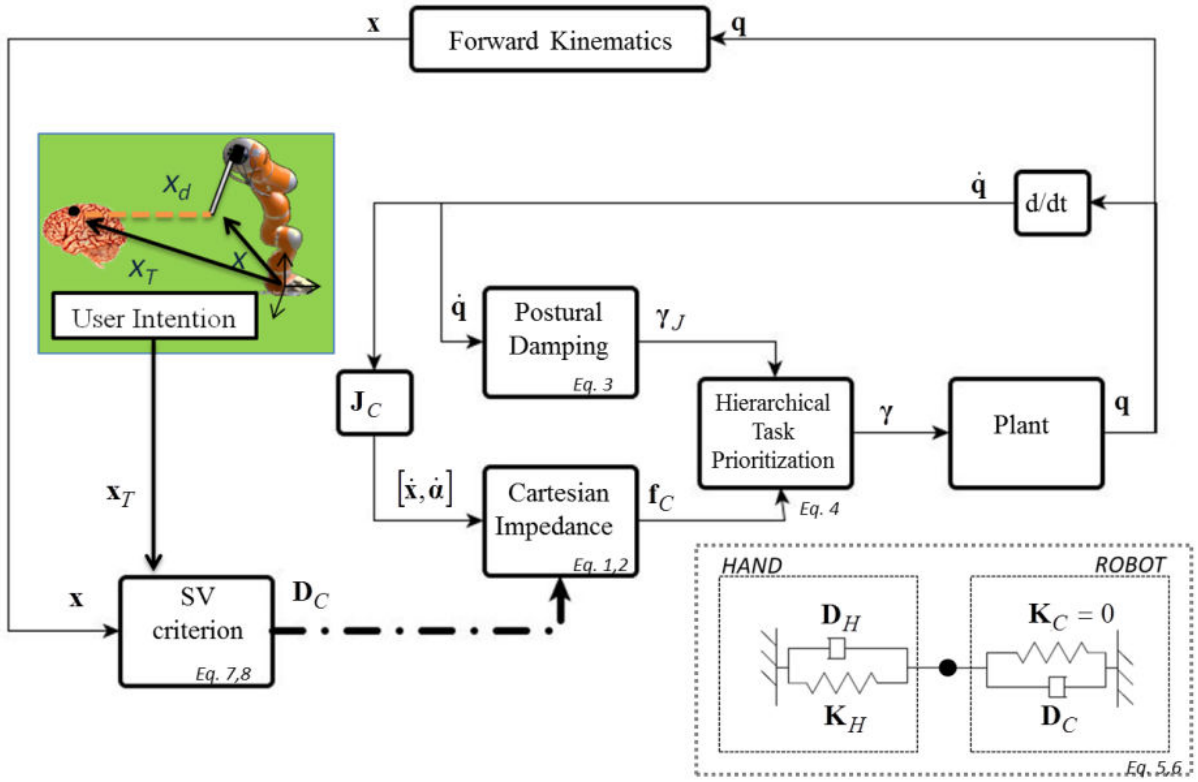

Figure 2. Scheme of the Space Variable damping controller and of the human-robot contact model. The hierarchical task prioritization approach combines the commands computed with the Cartesian impedance controller (null robotic stiffness $\mathbf{K}_C$) with the postural damping commands $\boldsymbol{\gamma}_J$ in the joint space. The Space Variable criterion varies the Cartesian damping parameter $\mathbf{D}_C$ depending on the actual position of the control point $\mathbf{x}$ and on the known position of the target $\mathbf{x}_T$. The actual Cartesian velocities ($\dot{\mathbf{x}}$, $\dot{\boldsymbol{\alpha}}$) are computed from the actual joint velocities ($\dot{\mathbf{q}}$) with the geometrical Jacobian $\mathbf{J}_C$. The gravitational and Coriolis-centrifugal terms of the feed-forward robot's dynamic compensation are not reported.

3. Methods

3.1 Impedance controlled robot model

During hands-on targeting execution, the robotic assistant must responsively react to the forces and torques applied by the operator when the tool is far away from the target, while increasing the resistance to the guidance motion during the final approach, thus improving the accuracy with which a target is intersected. An impedance controller in the task space [28] computes the desired Cartesian forces/torques $\mathbf{f}_C=[\mathbf{f}, \boldsymbol{\tau}]$ based on the predefined dynamic behaviour of the robot:

$$\mathbf{f} = \mathbf{K}_P\left(\mathbf{x}_d - \mathbf{x}\right) + \mathbf{D}_P\left(\dot{\mathbf{x}}_d - \dot{\mathbf{x}}\right) \tag{1}$$

$$\boldsymbol{\tau} = \mathbf{K}_R\left(\boldsymbol{\alpha}_d - \boldsymbol{\alpha}\right) + \mathbf{D}_R\left(\dot{\boldsymbol{\alpha}}_d - \dot{\boldsymbol{\alpha}}\right) \tag{2}$$

where $\mathbf{K}_C=[\mathbf{K}_P,\mathbf{K}_R]$ and $\mathbf{D}_C=[\mathbf{D}_P,\mathbf{D}_R]$ are the Cartesian stiffness and damping parameters of the arm, respectively, (prismatic (P) and rotational (R) components), $\mathbf{x}$ and $\mathbf{x}_d$ are the current and desired position of the control point and $\boldsymbol{\alpha}$ and $\boldsymbol{\alpha}_d$ are the current and desired orientation angles of the robot end effector. The dynamic of the robot is compensat-

ed with a feed-forward model-based torque controller, i.e., gravity and Coriolis-centrifugal terms.

In order to generalize the approach to redundant manipulators, the dynamic recursive null-space formulation [29] is used to combine Cartesian impedance behaviour with a damped posture strategy, in which the torque commands are computed as:

$$\gamma_J = -\mathbf{D}_J \dot{\mathbf{q}} \tag{3}$$

where $\dot{\mathbf{q}}$ is the actual joint velocity and $\mathbf{D}_J$ is the joint damping parameter. Thus, the combined torque commands are computed with the recursive null-space formulation as follows:

$$\gamma = \mathbf{J}_C{}^T \mathbf{f}_C + \mathbf{N}_C{}^T \gamma_J \tag{4}$$

where $\mathbf{J}_C$ is the Jacobian of the linear and angular Cartesian velocities at the control point and $\mathbf{N}_C = \mathbf{I} - \mathbf{A}^{-1}\mathbf{J}_C^T(\mathbf{J}_C\mathbf{A}^{-1}\mathbf{J}_C^T)^{-1}\mathbf{J}_C$ is the dynamically consistent null-space of $\mathbf{J}_C$ computed with the mass matrix $\mathbf{A}$ of the robot.

3.2 Interaction model

One of the theories about movement control is that the central nervous system guides joint movements through an equilibrium-point control [30], where the virtual point is determined by the muscle force used to maintain a limb position. Thus, a mass-spring-damper system can be used to model the dynamics of the user's hand on a single-point of contact during the interaction [31]. Supposing that the hand maintains contact with the manipulator at all times, the robot and the hand are at the same position ($\mathbf{x}$) and orientation ($\boldsymbol{\alpha}$).The coupled interaction model between the manipulator and the human hand, the dynamics of which are represented by the stiffness ($\mathbf{K}_H = [\mathbf{K}_{P,H}, \mathbf{K}_{R,H}]$) and damping ($\mathbf{D}_H = [\mathbf{D}_{P,H}, \mathbf{D}_{R,H}]$) matrices, is shown in Figure 2. The mass terms can be neglected (as in [32]) when a reasonable task bandwidth of 5Hz is considered in the damped case and the actual stiffness of the coupled system is given by the parallel equivalent of the two individual systems [33]. If the virtual stiffness of the manipulator is set to zero ($\mathbf{K}_C = 0$, not to become an additional load sensed during the cooperation [19]), the coupled interaction model can be approximated to:

$$\mathbf{f}_{ext} = \mathbf{K}_{P,H}(t) \cdot (\mathbf{x}_d - \mathbf{x}) - \left(\mathbf{D}_{P,H}(t) + \mathbf{D}_P\right)\dot{\mathbf{x}} \tag{5}$$

$$\boldsymbol{\tau}_{ext} = \mathbf{K}_{R,H}(t) \cdot (\boldsymbol{\alpha}_d - \boldsymbol{\alpha}) - \left(\mathbf{D}_{R,H}(t) + \mathbf{D}_R\right)\dot{\boldsymbol{\alpha}} \tag{6}$$

where the stiffness $\mathbf{K}_H$ and damping $\mathbf{D}_H$ parameters of the hand are unknown and time-varying. The estimation of the human arm's dynamics is not strictly required, because the damping characteristics of the hand is assumed to be implicitly adapted by the user to ensure passivity of the coupled system, which only depends on the applied human stiffness [33]. The manipulator's damping characteristic determines the degree of over-damped interaction during the assisted guidance.

3.3 Space Variable Damping Controller

In order to enhance human-robot interaction during hands-on robotic surgery, a variable damping controller varies the viscosity characteristics of the manipulator with the isotropic SV criterion, which is based on a priori knowledge of the surgical targeting gesture. Assuming that the target position is known in the robot base reference frame ($\mathbf{x}_T$), both the translational $\mathbf{D}_P$ and the rotational $\mathbf{D}_R$ damping matrixes will vary according to the distance between the actual position $\mathbf{x}$ of the control point and the known position of the target, so that higher damping is achieved only in areas of the robot workspace where high positional accuracy is required. A sigmoid spatial modulation is considered and applied independently in each direction of motion:

$$\mathbf{D}_P(d) = \underline{\mathbf{D}}_P + (\bar{\mathbf{D}}_P - \underline{\mathbf{D}}_P)\frac{1}{1 + e^{\beta(\|\mathbf{x}-\mathbf{x}_T\|-m)}} \tag{7}$$

$$\mathbf{D}_R(d) = \underline{\mathbf{D}}_R + (\bar{\mathbf{D}}_R - \underline{\mathbf{D}}_R)\frac{1}{1 + e^{\beta(\|\mathbf{x}-\mathbf{x}_T\|-m)}} \tag{8}$$

where $\underline{\mathbf{D}}_{P,R}$ and $\bar{\mathbf{D}}_{P,R}$ are the lower and upper boundaries of the translational and rotational damping parameters, respectively, m is a spatial threshold that defines the isotropic area around the target in which the damping is increased and β is a scalar parameter that defines the damping rate of change of the sigmoid function.

3.4 Experimental Protocol

The SV damping modulation criterion of the proposed controller was experimentally evaluated using the LWR4+ (Kuka, Augsburg, Germany), a seven-degrees-of-freedom flexible joint manipulator with joint torque sensors, which features 0.05mm repeatability (as per datasheet) and ≈1mm accuracy [34]. The effectiveness of the proposed SV damping controller was evaluated with respect to two constant isotropic damping controllers:

- Gravity compensation (GC): $\mathbf{D}_P = \underline{\mathbf{D}}_P = 0$Ns/m and $\mathbf{D}_R = \underline{\mathbf{D}}_R = 0$Nms/rad, i.e., a constant under-damped interaction; if the robot's dynamics were ideally compensated, the GC controller would allow the most transparent interaction with the user;

- Constant Optimal damping (CO): $\mathbf{D}_P = \bar{\mathbf{D}}_P$ =30Ns/m and $\mathbf{D}_R = \bar{\mathbf{D}}_R$ =30Nms/rad, i.e., a constant over-damped interaction; the robotic damping coefficient was computed to mimic the human arm damping effect ($\mathbf{D}_H = \sqrt{\mathbf{K}_H}$)[33], considering a mean human hand stiffness equal to 900N/m, according to the stiffness range defined in [31] during soft-normal-hard gripping.

The isotropic sigmoid spatial modulation (7)(8) of the SV controller was applied, varying the damping between the boundaries ($\underline{\mathbf{D}}_{P,R}$ and $\bar{\mathbf{D}}_{P,R}$) defined for the fixed parameter controllers. The spatial parameters of the SV criterion were heuristically determined during the repetitive execution of targeting gestures, according to the qualitative considerations of an expert user. Once the area of interest around the target was fixed (m equal to 50mm), the damping rate of change was determined as the maximum slope that guaranteed a perceived smooth dynamic modulation (β equal to 50m^{-1}). The above-mentioned control schemes were implemented as modules of the Whole Body Control library (Stanford) [35], i.e., a torque control framework with hierarchical task prioritization [29]. The robotic system was controlled in a real-time environment guaranteed by a Xenomai patched kernel (www.xenomai.org) with wrapper software modules implemented in the OROCOS and ROS frameworks (www.orocos.org, www.ros.org). Torque commands depending on the variable damping parameter were computed at 200Hz and internally updated at 1KHz from the LWR controller [28].

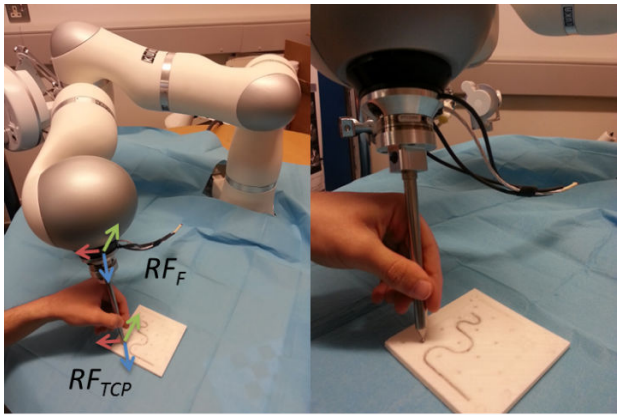

Figure 3. Experimental setup with the LWR4+ robot and the target calibration board. The reference frames of the robot flange (RT_F) and of the tool central point (RF_{TCP}) are also reported in RGB convention (red is x-axis, green is y-axis and blue is z-axis).

A bespoke linear tool was mounted on the robot flange, as shown in Figure 3. A reference frame with the origin coincident, with the tip of the linear tool and the z-axis coaxial with the tool's principal axis (RF_{TCP}), was defined with respect to the flange reference frame (RF_F) using a pivoting procedure. Tests were performed on a calibration board, mimicking the target approaching gestures of an open-skull neurosurgical procedure. The board was realized with a rapid prototyping machine (accuracy 0.5mm) and a 4x4 grid of 2cm equally spaced points was realized on the surface, together with five 3mm diameter calibration divots. The user's motion intentions were constrained to provide a ground truth for the evaluation of the controllers' performance: one of the grid points was chosen as the intended target of the assisted gesture and its position in the robot base reference frame $\mathbf{x}_T$ was computed through a rigid registration procedure [36] on the board divots (fiducial registration error [37] equal to 1.1mm). Fifteen non-expert users were asked to perform 12 robotic assisted targeting gestures towards the predefined target on the calibration board, with each of the three GC, CO and SV controllers in a randomized order. Users (11 right-handed, four left-handed) were asked to use their dominant hand to perform the cooperative tasks. During each trial, the initial joint positions of the manipulator were varied randomly both in terms of the Cartesian pose RF_{TCP} (distance from target greater than 300mm) and the position of the elbow, in order to evaluate the controllers in arbitrary dynamic configurations.

3.5 Performance Indexes

During the randomized trials, the joint configurations, the Cartesian pose of the TCP and the exerted Cartesian forces estimated from the external joint torques (low pass filter with cut-off frequency between 100-300Hz) were provided by the internal KUKA controller (at 200Hz). The time derivatives of the Cartesian TCP position, e.g., Cartesian velocities, were computed with a best-fit first order adaptive window recursive filter [38]. Based on this information, the performances of the constant and variable damping controllers were evaluated in terms of:

- target pointing error (E_T), computed as the root mean square distance between the actual TCP position and the known calibrated target position evaluated at the end of the motion (window equal to 0.5s);
- target approaching execution time (T), evaluated starting from a 100mm distance from target to compensate for different initial path length;
- mean norm of the exerted Cartesian forces (F_{mean}) during the cooperation, in order to quantify the transparency of the system and thus the user's efforts;
- maximum norm of the acceleration (Acc) computed at the contact point during the cooperation, in order to quantify the reaction capabilities of the system;
- zero crossing index (ZC), evaluated according to the velocity measured at the TCP when the distance from the target was less than 10mm, in order to quantify the number of speed direction changes experienced while approaching the target;
- motion smoothness (S), evaluated as the inverse of the root mean square jerk, i.e., third derivative of the TCP positions when approaching the target (distance from the target less than 100mm).

The mean behaviour of each user was evaluated during the gesture execution with the GC, CO and SV controllers over 10 trials (the first and second trials were excluded in order to account for user's accommodation). For each user, the median value and the first and third interquartile ranges (IQR 25%; IQR 75%), as well as the mean and standard deviations were computed over different trials, respectively, for the discrete ZC index and all other performance indexes. A comparative analysis of the performance of the GC, CO and SV controllers among different users was carried out using the Friedman paired test and Bonferroni-Holm correction ($p<0.05$).

4. Results

Evaluation of the performance indexes for the assisted targeting gestures is reported in Figure 4. The target pointing error (Figure 4a) of the CO and SV controllers (mean value below 1.5 mm) is comparable to the experimental accuracy of the LWR4+ manipulator reported for repetitive motions [34], while the accuracy of the GC controller is significantly reduced (by almost 50%), resulting in a mean target pointing error equal to 2.2mm. The approaching execution time (Figure 4b) computed on the last 100mm towards the target is comparable among all three controllers (mean value around 6s). Figure 4c shows that the mean norm of the exerted forces applied during the cooperative interaction with the SV controller (mean value equal to 2.6N) are greater than for the GC controller (mean value equal to 1.2N) and reduced with respect to the CO controller (mean value equal to 4.1N). As shown in Figure 4d, the accelerations allowed while cooperating with the SV controller are comparable to those for the GC controller (mean value greater than $1m/s^2$) and significantly higher (around 50%) with respect to the CO controller (mean value below $0.5\ m/s^2$). At the same time, the trajectory smoothness (Figure 4e) and the zero crossing index (Figure 4f) of the SV controller are comparable to those of the CO controller (respective mean smoothness greater than $0.8s^3/m$ and median direction changes equal to 4), and reduced by more than 30% with respect to the GC controller (respective mean smoothness below $0.6s^3/m$ and median direction changes equal to 6).

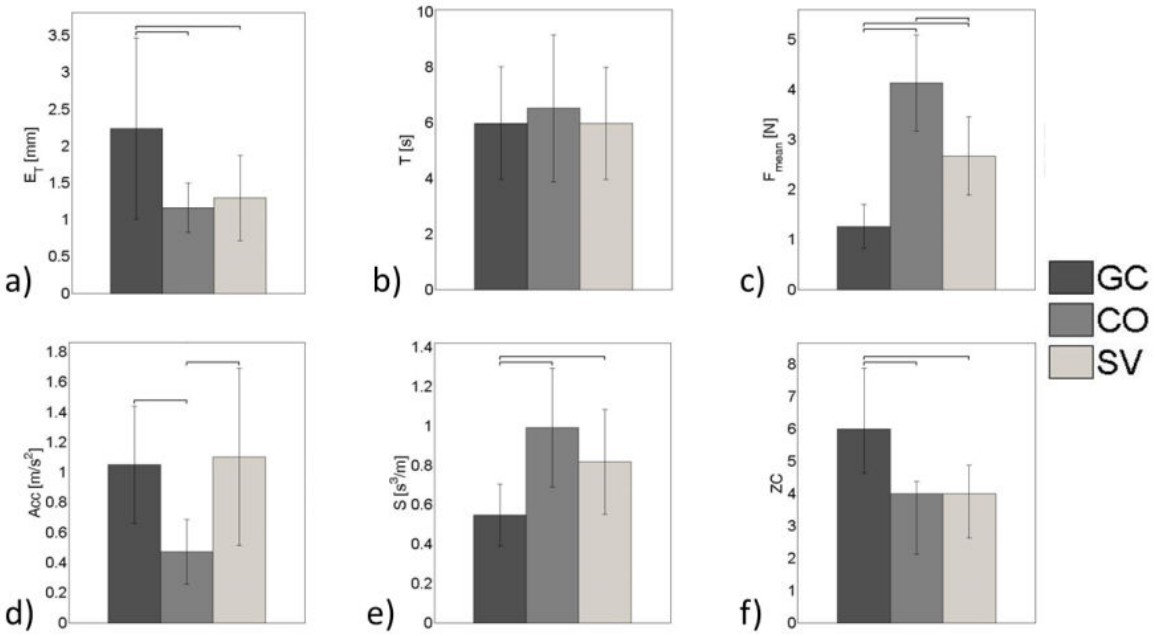

Figure 4. Evaluation of a) pointing accuracy (E_T); b) target approaching execution time (T); c) mean norm of the exerted Cartesian force at the contact point (F_{mean}); d) maximum norm of the acceleration at the contact point (Acc); e) motion smoothness (S); f) zero crossing (ZC) of the three controllers (GC,CO, SV) among the randomized users' group. Vertical bars represent mean and standard deviations for each population of the indexes (a)-(e) and median values and quartiles (25% and 75%) for the population of index (f). Horizontal lines represent statistically significant differences, as determined by the Friedman paired test ($p<0.05$) with the Bonferroni-Holm correction.

5. Discussion

A hands-on variable damping controller is presented to enhance human-robot interaction during targeting gestures, particularly aimed at surgical applications. Based on the assumption that the desired position at the end of the assisted motion is known a priori, the space variable criterion allows one to modulate the viscosity parameter of the manipulator along the trajectory and thus to smoothly vary the level of transparency and pointing accuracy of the robotic system according to the target position. During robotic surgical interventions, this assumption is usually verified by the registration procedures that are performed between the intra-operative space, the robot space and the patient-specific image space [9,10], which localize the area of intervention of the patient in the robot base reference

frame. Nevertheless, during brain cortex stimulation in open-skull neurosurgery [12], the stimulation site on the exposed brain cortex is not known a priori in the pre-operative phase or for changes occurring during the procedure, depending on the surgeon's stimulation intentions. In this context, a possible application scenario of the SV controller is proposed for brain cortex stimulation procedures, where the surgeon/user is able to configure the damping field of the SV criterion online, based on his/her actual motion intention using an image-guided navigation system.

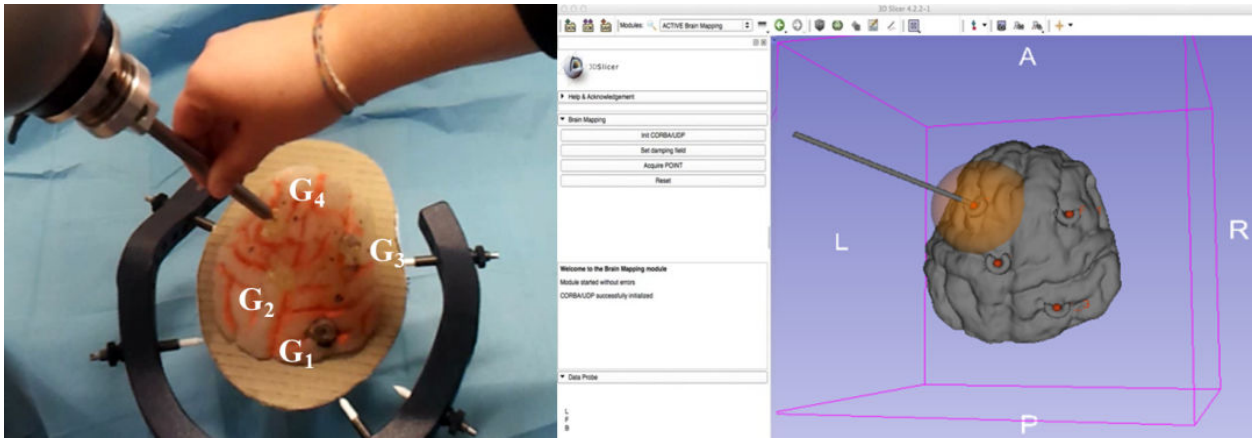

Figure 5. Qualitative feasibility study for applying the SV approach for brain cortex stimulation procedures in neurosurgery: left) the brain phantom was fixed with respect to the robot's base and registered to the preoperative images with a correspondent point registration procedure on four gadolinium markers (G1-4); right) navigation of the surgical tool (grey cylinder) on the 3D model of the brain phantom and the GUI implemented to interactively set the damping field (yellow sphere represents the spatial threshold m of the sigmoid) and for acquiring the stimulation points (red dots) during the cooperative procedure.

Thanks to the dynamic modulation provided by the SV controller, an area of surgical interest – including multiple indented stimulation sites – can be defined within a single damping field. A qualitative feasibility study was performed on a brain phantom, the specific MRI-CT images of which were processed and segmented to build the 3D model of the brain surface in the open-source 3D Slicer software (http://www.slicer.org) [39]. As shown in Figure 5, a custom-made graphical user interface (GUI) was used to acquire the position of the intended surgical target online, computed as a point 5cm away along the *z*-axis from the current TCP pose; the damping field was then set accordingly.

The SV controller isotropically varies both the translational and rotational damping parameters of the manipulator within a predefined range of values. The user's hand is hypothesized to behave as a spring-damper system with time-variable dynamic parameters [31]. Thus, it is realistic to assume that the damping characteristics of the hand are adapted by the user to ensure passivity of the coupled system in relation to the applied human stiffness.

The effectiveness of the proposed SV controller was experimentally evaluated on a pool of 15 non-expert users with respect to both gravity compensation (0Ns/m, 0Nms/rad) and constant optimal (30Ns/m, 30Nms/rad) damping controllers, the transparency and pointing accuracy of which are maximized, respectively. The experimental tests were performed using a registered calibration board, on which the surgical target was defined and visible to the users, thus constraining the user's pointing intention to be considered as the motion ground truth. The presented protocol is the first necessary step for evaluating the performance of the proposed controller under laboratory conditions.

Experimental results showed that the performance of the proposed controller combined the positive features of an optimal damping controller, i.e., high pointing accuracy (mean target localization error of approximately 1.5mm) and intuitive convergence to the target (the direction changes are reduced by a factor of 30% with respect to the constant under-damped scenario), and of the gravity compensation controller, i.e., high reaction capabilities (acceleration increased by more than 30% with respect to the constant over-damped scenario). Although reduced with respect to the GC controller, the transparency of the system with the SV controller (mean exerted force below 3N) is increased by 40% with respect to the CO controller. Thus, the SV controller allows for reducing the user's efforts without affecting the performance of accuracy and execution time, which are crucial aspects for the clinical acceptability of the system. It has to be noted that no substantial improvement of the execution time index was shown on the final segment of the guidance trajectory (100mm distance from target), but a significant reduction with respect to the CO controller is nonetheless expected on longer paths, e.g., motions from/to the resting configuration of the manipulator. The smoothness of the assisted trajectory (mean jerk below $1m/s^3$) is guaranteed for all three controllers. Moreover, the experimental validation demonstrates the reliability of the SV controller with

respect to the non-ideality of the dynamic model-based torque controller and to the time-varying human interaction during the cooperation.

So as to be applied to a redundant manipulator, the SV control approach was defined in the framework of the hierarchical task prioritization [35] and combined with a posture damping strategy to control the position of the robotic elbow during the assisted cooperation. The investigation of the potential benefits derived from different null-space control strategies, e.g., the minimization of the residual robot inertia, was not the focus of this work and will be addressed in the future.

6. Conclusion

This paper outlines the development of a space variable controller that was shown to be suitable for cooperative surgical tasks that require different levels of positional accuracy in the operating field, such as targeting gestures during brain cortex stimulation in open-skull neurosurgery [12]. Enhanced performance was demonstrated via comparison to a number of fixed parameter controllers, where reaching tasks under laboratory conditions resulted in reduced targeting errors and decreased user effort. Future work will address enhancement of the hands-on controller, which combines the SV criterion with other human-like adaptation criteria, both for free-motion guidance and for soft tissue interaction. Additionally, performance evaluation will be carried out with a pool of expert surgeons on brain-mimicking phantoms to specifically assess the effectiveness of the proposed SV controller for brain cortex stimulation procedures during robotic neurosurgery.

7. Acknowledgements

The authors would like to thank Kuka Industries for providing the inverse dynamic model of the LWR4+ and for their technical support. Special thanks to Dr Cardinale and Dr Marras for the clinical support and to Josh Petersen and Emilia Ambrosini for their help during the experimental validation. This work was founded by the FP7 ACTIVE project (FP7-ICT-2009-6-270460) and by the Scuola Interpolitecnica di Dottorato.

8. References

[1] Comparetti MD, De Momi E, Beyl T, Kunze M, Raczkowsky J, Ferrigno G (2014) Convergence Analysis of an Iterative Targeting Method for Keyhole Robotic Surgery. Int. J. Adv. Robot. Syst. 11:60.

[2] Li C, Wang T, Hu L, Zhang L, Du H, Wang L et al. (2014) Accuracy Analysis of a Robot System for Closed Diaphyseal Fracture Reduction. Int. J. Adv. Robot. Syst. 11:169.

[3] Ripel T, Krejsa J, Hrbacek J, Cizmar I (2014) Active Elbow Orthosis. Int. J. Adv. Robot. Syst. 11:143.

[4] Zollo L, Salerno A, Vespignani M, Accoto D, Passalacqua M, Guglielmelli E (2013) Dynamic Characterization and Interaction Control of the CBM-Motus Robot for Upper-Limb Rehabilitation. Int. J. Adv. Robot. Syst. 10:374.

[5] Singer SM, Akin DL (2011) A Survey of Quantitative Team Performance Metrics for Human-Robot Collaboration. Int Conf on Environmental Systems. 2001; 5248:AIAA.

[6] Jarrassé N, Paik J, Pasqui V, Morel G (2008) How can human motion prediction increase transparency?. Int. Conf. on Robotics and Automation. 2008; pp. 2134-2139.

[7] Pearle AD, Kendoff D, Stueber V, Musahl V, Repicci JA (2009) Perioperative management of unicompartmental knee arthroplasty using the MAKO robotic arm system (MAKOplasty). Am J Orthop. 38(2):16-19.

[8] Kazanzides P, Zuhars J, Mittelstadt B, Taylor RH (1992) Force sensing and control for a surgical robot. Int. Conf. on Robotics and Automation. 1992; pp. 612-617.

[9] Ferrand-Sorbets S, Taussig D, Fohlen M, Bulteau C, Dorfmuller G, Delalande O (2010) Frameless stereotactic robot-guided placement of depth electrodes for stereo-electroencephalography in the presurgical evaluation of children with drug-resistant focal epilepsy. CNS Annual Meeting. 2010.

[10] Hughes G, Vadera S, Bulacio J, Gonzalez-Martinez J (2012) Robotic placement of intracranial depth electrodes for long-term monitoring: Utility and efficacy. ASSFN Biennial Meeting 2012.

[11] De Lorenzo D, Koseki Y, De Momi E, Chinzei K, Okamura AM (2013) Coaxial Needle Insertion Assistant With Enhanced Force Feedback. IEEE T Bio-Med Eng. 60(2):379-389.

[12] Szelenyi A, Bello L, Duffau H, Fava E, Feigl GC, Galanda M, Neuloh G, Signorelli F, Sala F, Workgroup for Intraoperative Management in Low-Grade Glioma Surgery within the European Low-Grade Glioma Network (2010) Intraoperative electrical stimulation in awake craniotomy: methodological aspects of current practice. Neurosurg Focus. 28:E7.

[13] Burdet E, Osu R, Franklin DW, Milner TE, Kawato M (2001) The central nervous system stabilizes unstable dynamics by learning optimal impedance. Nature. 414:446–449.

[14] Kadiallah A, Franklin DW, Burdet E (2012) Generalization in adaptation to stable and unstable dynamics. PLoS one. 7:10.

[15] Ganesh G, Albu-Schaffer A, Haruno M, Kawato M, Burdet E (2010) Biomimetic motor behavior for simultaneous adaptation of force, impedance and

trajectory in interaction tasks. Int. Conf. on Robotics and Automation. 2010; pp. 2705-2711.

[16] Ganesh G, Jarasse N, Haddadin S, Albu-Schaeffer A, Burdet E (2012) A versatile biomimetic controller for contact tooling and tactile exploration. Int. Conf. on Robotics and Automation. 2012; pp. 3329-3334.

[17] Yang C, Ganesh G, Haddadin S, Parusel S, Albu-Schaeffer A, Burdet E (2011) Human like adaptation of force and impedance in stable and unstable interactions. IEEE T Robot. 27(5):918–930.

[18] Kronander K, Billard A (2013) Learning Compliant Manipulation through Kinesthetic and Tactile Human-Robot Interaction. IEEE Trans Haptics. 7(3): 367-380.

[19] Ikeura R, Inooka H (1995) Variable impedance control of a robot for cooperation with a human. Int. Conf. on Robotics and Automation. 1995; pp. 3097–3102.

[20] Ikeura R, Moriguchi T, Mizutani K (2002) Optimal variable impedance control for a robot and its application to lifting an object with a human. Int. Symp. on Robot and Human Interactive Communication. 2002; pp. 500–505.

[21] Erden MS, Marić B (2011) Assisting manual welding with robot. Robot Cim-Int Manuf. 27(4):818-828.

[22] Duchaine V, Gosselin CM (2007) General Model of Human-Robot Cooperation Using a Novel Velocity Based Variable Impedance Control. World Haptics Conf. 2007; pp. 446-451.

[23] Tsetserukou D, Tadakuma R, Kajimoto H, Kawakani N, Tachi S (2007) Intelligent variable joint impedance control and development of a new whole-sensitive anthropomorphic robot arm. Int. Symp. on computational intelligence in robotics and automation. 2007; pp. 338–343.

[24] Tsumugiwa T, Yokogawa R, Hara K (2002) Variable impedance control based on estimation of human arm stiffness for human-robot cooperative calligraphic task. Int. Conf. on Robotics and Automation. 2002; pp. 644–650.

[25] Duchaine V, St-Onge BM, Gao D, Gosselin C (2012) Stable and Intuitive Control of an Intelligent Assist Device. IEEE Trans Haptics. 5(2):148-159.

[26] Nishiwaki K, Yano K (2008) Variable impedance control of meal assistance robot using potential method. Int. Conf. on Intelligent Robots and Systems. 2008; pp. 3242–3247.

[27] Ikeura R, Mizutani K (1998) Control of Robot Cooperating with Human Motion. Int. Workshop on Robot and Human Communication. 1998; pp. 525-529.

[28] Albu-Schaffer A, Ott C, Hirzinger G (2004) A passivity based Cartesian impedance controller for flexible joint robots - part ii: fullstate feedback, impedance design and experiments. Int. Conf. on Robotics and Automation. 2004; pp. 2666–2672.

[29] Sentis L, Khatib O (2005) Synthesis of whole-body behaviors through hierarchical control of behavioral primitives. Int. J. Hum. Robot. 2(4):505–518.

[30] Bizzi E, Hogan N, Mussa-Ivaldi FA, Giszter S (1992) Does the nervous system use equilibrium-point control to guide single and multiple joint movements. Behav. Brain Sci. 15:603-613.

[31] Marayong P, Hager GD, Okamura AM (2006) Effect of hand dynamics on virtual fixtures for compliant human-machine interfaces. Int. Symp. on Haptic Interfaces for Virtual Environments and Teleoperator Systems. 2006; pp. 109–115.

[32] Roveda L, Vicentini F, Molinari Tosatti L (2013) Deformation-Tracking Impedance Control in Interaction with Uncertain Environments. Int. Conf. on Intelligent Robots and Systems. 2013; pp. 1992-1997.

[33] Duchaine V, Gosselin CM (2008) Investigation of human-robot interaction stability using Lyapunov theory. Int. Conf. on Robotics and Automation. 2008; pp. 2189-2194.

[34] Stein D, Monnich H, Raczkowsky J, Worn H (2009) Visual servoing with an optical tracking system and a lightweight robot for laser osteotomy. Int. Conf. on Control and Automation. 2009; pp. 1896–1900.

[35] Philippsen R, Sentis L, Khatib O (2011) An Open Source Extensible Software Package to Create Whole-Body Compliant Skills in Personal Mobile Manipulators. Int. Conf. on Intelligent Robots and Systems. 2011; pp. 1036-1041.

[36] Horn BKP (1987) Closed-form solution of absolute orientation using unit quaternions. J. Opt. Soc. Amer. A. 4(4):629-642.

[37] Fitzpatrick JM, West JB (2001) The Distribution of Target Registration Error in Rigid-Body Point-Based Registration. IEEE T Med Imaging. 20(9): 917-927.

[38] Janabi-Sharifi F, Hayward V, Chen CSJ (2000) Discrete-time adaptive windowing for velocity estimation. IEEE Trans. Control Syst. Technol. 8(6): 1003-1009.

[39] Fedorov A, Beichel R, Kalpathy-Cramer J, Finet J, Fillion-Robin JC, Pujol S, Bauer C, Jennings D, Fennessy F, Sonka M, Buatti J, Aylward SR, Miller JV, Pieper S, Kikinis R (2012) 3D Slicer as an Image Computing Platform for the Quantitative Imaging Network. Magn Reson Imaging. 30(9):1323-41. PMID: 22770690.